Effects of piezopotential spatial distribution on local contact dictated transport property of ZnO micro/nanowires

Yan Zhang,[1,2] Youfan Hu,[1] Shu Xiang,[1] and Zhong Lin Wang[1,a)]
[1]*School of Material Science and Engineering, Georgia Institute of Technology, Atlanta, Georgia 30332-0245, USA*
[2]*Institute of Theoretical Physics, Lanzhou University, Lanzhou 730000, People's Republic of China*

(Received 9 June 2010; accepted 4 July 2010; published online 23 July 2010)

We present a study on the effect of deformation induced piezoelectric potential (piezopotential) in a ZnO micro/nanowire on its electrical transport properties by choosing different contacting locations on the wire to form a metal-ZnO contact. When a ZnO wire is under nonuniform deformation, the local piezopotential distribution at different positions shows significant effect on and distinct trend of variation in the charge carrier transport characteristic. This study has a broad impact on understanding the characteristics of piezotronic devices based on nanowires of wurtzite materials by controlling local contact position and contact size. © *2010 American Institute of Physics*. [doi:10.1063/1.3467815]

Bulk piezoelectric materials have shown great and broad applications as transducers and sensors. At nanoscale, piezoelectric-semiconductive nanowires of ZnO, GaN, InN, and ZnS are the fundamental building blocks for fabricating a range of nanodevices.[1–4] Typically, owning to the coupling of piezoelectric and semiconducting properties, various unique piezotronic nanodevices have been fabricated based on ZnO micro/nanowires, including nanogenerators,[5–7] piezoelectric field effect transistors,[8] piezoelectric diodes,[9] piezoelectric chemical sensors,[10] and most recently, the piezophototronic devices.[11,12] Piezopotential, which plays an important role in the above devices, has a spatial distribution in the micro/nanowires depending on the applied tensile, compressive and/or deflecting force, which induces a nonuniform distribution in strain. Owing to the small size of the nanowires, strain introduced in fabrication is inevitable. We typically have two ideal cases. For a ZnO/GaN nanowire nanogenerator that is transversely pushed by a conductive atomic force microscopy (AFM) tip, the stretched side and the compressed side surfaces exhibit a positive and negative piezopotential, respectively.[5,13,14] Another alternative geometry of the nanogenerator is a simple two ends bonded single wire, with the external force uniformly acting on the nanowire in the direction parallel to the nanowire (c-axis direction).[15] In both configurations, piezopotential will drive transient flow of electrons when the deformation is periodically induced. The piezopotential induced in the nanowire can significantly tune the Schottky barrier heights (SBHs) at the metal-nanowire contacts,[16] and such a tuning effect is nonsymmetric at the two contacting ends due to the gradient of the piezopotential.[11,17] In practice, however, a nanowire can be strained along and deflected perpendicular to its axis. Such a nonuniform spatial distribution of piezopotential is likely to affect the performance of the piezotronic devices.

In this paper, we study the effect of the piezopotential spatial distribution on the local charge transport characteristic at the contact.

To be simple and most plausible, the ZnO micro/nanowire is assumed to grow along the c axis with length of $l=10$ μm and radius of $a=0.5$ μm [Fig. 1(a)]. Although a circular cross-sectional beam is proposed in Fig. 1(a), the presented methodology applies to nanowires of arbitrary cross-sections. In general, the externally applied force can be decomposed into vertical and parallel components in reference to the wire's direction. Using the finite element method (FEM), we calculate the distribution of the piezopotential in the ZnO micro/nanowires with a vertical force $\vec{F}_x$ and parallel external force $\vec{F}_z$, as shown in Fig. 1(a). For simplicity, we ignored the finite doping in the nanowire, thus its electrical conductance is neglected. According to our previous studies,[13–15,17,18] the two components of the applied forces are chosen as $\vec{F}_x=-1000$ nN and $\vec{F}_z=-500$ nN. Figure 1(a) shows the distribution of piezopotential in the nanowire at its side cross-section parallel to its axis. The piezopotential at

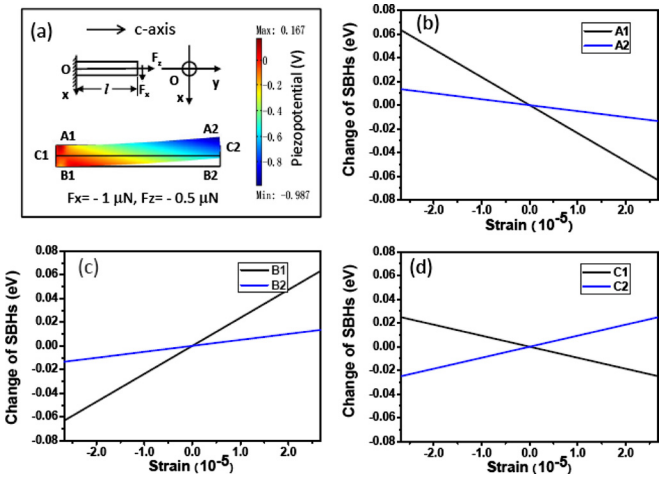

FIG. 1. (Color online) (a) Schematic of a ZnO cantilever beam and its cross-section, as well as the calculated piezopotential distribution in a one-end fixed ZnO cantilever beam under strain using the FEM. The color represents the local piezopotential in unit of volt; the arrowhead indicates the strain increase direction. Predicted change in SBHs for the devices with electrical contact at positions at A1 and A2 (b), B1 and B2 (c), and (d) C1 and C2, respectively.

a)Author to whom correspondence should be addressed. Electronic mail: zlwang@gatech.edu.

points A1 and A2 decreases with increase in vertical force component, while it increases at points B1 and B2 under the same condition; for the positions at C1 and C2, the piezopotential, which is largely determined by the parallel force component, increases at one end, and decreases at the other end with the increase in the tensile force. For a metal-semiconductor-metal back-to-back Schottky contacted ZnO micro/nanowire device, the changing of piezopotential tunes the effective heights of the Schottky barriers at the electrical contact. As a result, the characteristic of I-V transport measured depends sensitively on where the positions of the electrical contacts being made.

Now we begin to describe the change in SBHs related to the piezopotential variation if we fabricate electrical contact at different positions at the nanowire. Assuming a small uniform mechanical strain S_{jk},[19] we can write the polarization P vector in terms of strain S as follows:

$$(\mathrm{P})_i = (\mathrm{e})_{ijk}(\mathrm{S})_{jk}, \tag{1}$$

where the third order tensor $(\mathrm{e})_{ijk}$ is the piezoelectric tensor. According to the conventional theory of piezoelectric and elasticity,[13,14,20,21] the constituter equations can be written as follows:

$$\begin{cases} \sigma = \mathrm{c_E S} - \mathrm{e^T E} \\ \mathrm{D} = \mathrm{eS} + \mathrm{kE} \end{cases}, \tag{2}$$

where σ is the stress tensor, E is the electric field, D is the electric displacement, $\mathrm{c_E}$ is the elasticity tensor, and k is the dielectric tensor. The material elastic constants are approximated to be the isotropic elastic modulus E and Poisson ratio ν, and obtain the solutions of stress by Saint–Venant theory of bending.[14,21] Along the x axis, the stress can be expressed as follows:

$$\begin{cases} (\tau_{31})_{x=0} = \dfrac{(3+2\nu)}{8(1+\nu)}\dfrac{F_x a^2}{I_y}\left(1 - \dfrac{1-2\nu}{3+2\nu}\dfrac{y^2}{a^2}\right), \\ (\tau_{23})_{x=0} = 0 \\ (\tau_{33})_{x=0} = \dfrac{F_z}{\pi a^2} \end{cases} \tag{3}$$

Thus, we can obtain the piezoelectric polarization on the electrical contact as follows:

$$\begin{cases} P_x = \dfrac{2F_x}{\pi a^2 E} e_{15}(1+2\nu) \\ P_y = 0 \\ P_z = \dfrac{F_z}{\pi a^2 E}(2\nu e_{31} - e_{33}) \end{cases}, \tag{4}$$

where a is the radius of the wire, e_{15}, e_{31}, and e_{33} are the piezoelectric constants. The effect of piezoelectric polarization on the electrical contact will shift the Fermi level at the interface and modify the charge distribution profile, which subsequently affect the SBH. The change in SBH by piezoelectric polarization is given approximately by the following:[16]

$$\Delta\phi_B = \frac{\sigma_{\mathrm{pol}}}{D}\left(1 + \frac{1}{2q_s w_d}\right)^{-1}, \tag{5}$$

where σ_{pol} is the volume density of the polarization charges (in units of the electron charge q), which is given by: $\sigma_{\mathrm{pol}} = -\vec{n}\cdot\vec{P}/q$, $\vec{n}$ is the unit vector along normal direction of the device surface, D is a two-dimensional density of interface states at the Fermi level in the semiconductor band gap at the Schottky barrier, and w_d is the width of the depletion layer. Associated with the states in the band gap at the interface is a two-dimensional screening parameter $q_s = (2\pi q^2/\kappa_0)D$. In the last relationship, q is the electronic charge and κ_0 is the dielectric constant of the semiconductor. Substituting Eq. (4) into Eq. (5), we obtain

$$\Delta\phi_B = -\frac{4\pi q w_d\{2(\vec{n}_x\cdot\vec{F}_x)e_{15}(1+2\nu) + (\vec{n}_z\cdot\vec{F}_z)(2\nu e_{31} - e_{33})\}}{\kappa_0(1 + 2(2\pi q^2/\kappa_0)Dw_d)\pi a^2 E}. \tag{6}$$

It is very important that if we neglect the parallel component $\vec{F}_z$, from Eqs. (4) and (6), the result agrees with the results of single ZnO/GaN nanowire nanogenerator that is transversely pushed by a conductive AFM tip. With $\vec{F}_x = 0$, then this model is the working principle of two-end bonded nanowire based nanogenerator, piezoelectric diodes and piezophototronic device. From Eq. (6), the different position of the electrical contact is likely to affect the characteristics of the piezotronic devices. For the two-dimensional density of interface states D, in a large range from 1×10^{13} to 1×10^{18} $(\mathrm{eV\ cm^2})^{-1}$, the condition of $2(2\pi q^2/\kappa_0)Dw_d \ll 1$ always hold. Thus, Eq. (6) can be rewritten as follows:

$$\Delta\phi_B = -\frac{4\pi q w_d\{2(\vec{n}_x\cdot\vec{F}_x)e_{15}(1+2\nu) + (\vec{n}_z\cdot\vec{F}_z)(2\nu e_{31} - e_{33})\}}{\kappa_0\pi a^2 E}. \tag{7}$$

Then, if $w_d = 20$ nm, which is the typical value obtained from the experiments, $E = 129.0$ GPa, and $\upsilon = 0.349$, the trend of SBHs at different positions on the wire in responding to the applied strain can be obtained, as shown in Figs. 1(b)–1(d). First of all, the change in SBHs has a linear relationship with strain, which agrees well with experimental data.[17] If the electrical contact is at positions A1 and A2, both the SBHs will decrease with increasing strain but possessing different changing rate, as shown in Fig. 1(b). For contacting positions at B1 and B2, as shown in Fig. 1(c), we notice that the linear relations of the SBHs with strain have positive slope but with different magnitudes; the result has a reversed trend comparing to that for contacting positions at A1 and A2. The change in SBHs on the electrical contact at C1 and C2 as plotted in Fig. 1(d) shows that the SBH at contact position C1 decreases and at C2 increases with increasing strain. This entirely different SBHs changes at different contacting positions will have remarkable effect on the devices transport properties.

Three kinds of device were designed to present the idea, as shown in Fig. 2(a). The first one is the top electrode configuration. A ZnO microwire was first laid down on a polystyrene (PS) substrate, and then each end of the wire was fixed to the substrate using silver paste. This configuration corresponds to the case of making contacts at position A1 and A2. The second kind is the bottom electrode configuration. For this kind of device, a ZnO microwire was laid down on predefined electrodes on a Kapton film, and then the film will be attached to a PS substrate for manipulation. The microwire will be fixed to the Kapton film by the van der Waals' force. This corresponds to the case of making electri-

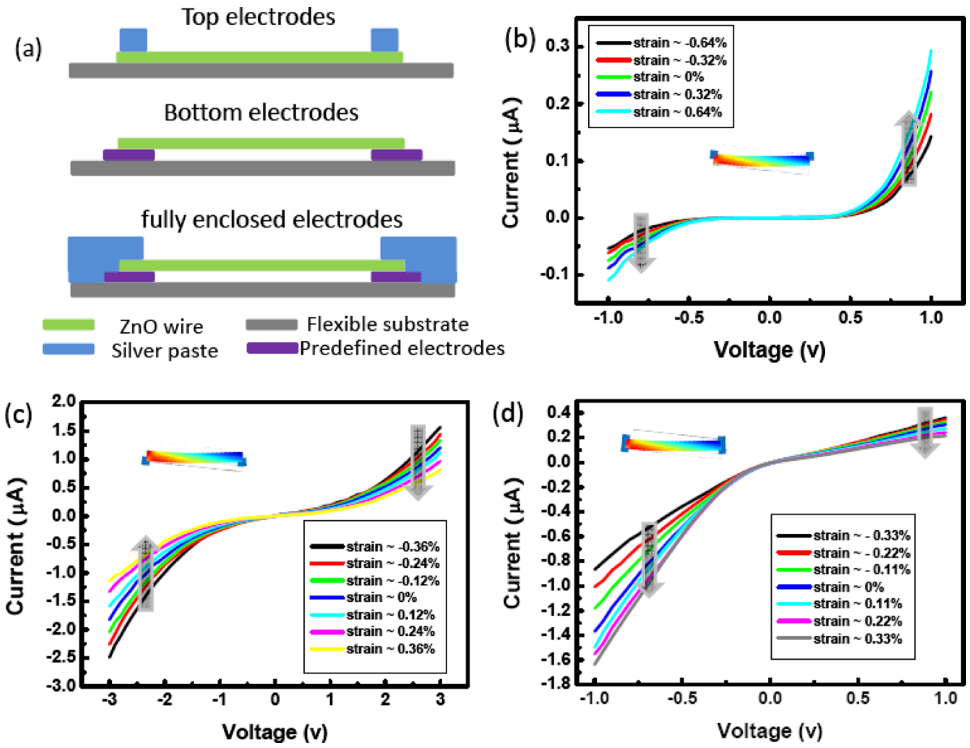

FIG. 2. (Color online) (a) Schematic of three kinds of contact configurations to be examined experimentally, and the corresponding I-V characteristics as a function of the applied strain are to be presented in [(b)–(d)], respectively. (b) For the top electrode configuration, current increases in the entire voltage range with increasing of strain but with different increasing rate in the negative and positive voltage ranges; (c) for the bottom electrode configuration, the current decreases in the entire voltage range with the increase in strain but with different changing rate in the negative and positive voltage ranges; (d) for the fully enclosed electrode configuration, the current increases in the negative and decrease in the positive voltage range as the strain increases. The arrowheads indicate the trend of current change with the increase in the applied strain. The insets in (b)–(d) are the corresponding contacting configurations with the distribution of the strain presented.

cal contact at positions B1 and B2. We called the third kind as fully enclosed electrodes configuration, which is the most conventional case. Comparing to the second kind of contact, the third one adds a silver paste covering the end of the microwire on the predefined electrode, making the end of the microwire fully surrounded by metal electrode. The electrical potential distribution on the side wall of the microwire cancels on average, and only the potential at the end surface has effect. This corresponds to the case of making contact at positions C1 and C2. For all of the devices, an additional very thin layer of polydimethylsiloxane was used to package the entire device, and it kept the device mechanically robust under repeated manipulation. The strain was introduced via bending the substrate by a precisely controlled linear stage with a motion resolution of 0.0175 μm. The piezoresponse of these three kinds of devices is shown in Figs. 2(b)–2(d), respectively. For the top electrode configuration, according to the classic thermionic emission-diffusion theory,[22] the change trend of SBHs at position A1 and A2 as showed in Fig. 1(b), will result in a current increase with increasing strain in the whole voltage range but with different increasing rate in the negative and positive voltage ranges. Besides of this, a nonsymmetrical change in I-V curves in the positive and negative voltage ranges was observed, as predicated theoretically. For the device with bottom electrodes configuration, corresponding to the SBHs variation shown in Fig. 1(c), the current is decreased in the whole voltage range when the applied strain is increased, and a nonsymmetrical variation characteristics were also observed due to the different positive slopes at contact position B1 and B2. When the fully enclosed electrodes are used, a pure nonsymmetrical change in I-V curves is observed, as shown in Fig. 2(d).

Research supported by NSF (Grant Nos. DMS 0706436, CMMI 0403671, and ENG/CMMI 112024), BES DOE (Grant No. DE-FG02-07ER46394), Airforce. Yan Zhang and Youfan Hu contributed equally to this work.

[1]Z. W. Pan, Z. R. Dai, and Z. L. Wang, Science **291**, 1947 (2001).
[2]C. M. Lieber and Z. L. Wang, MRS Bull. **32**, 99 (2007).
[3]W. Lu and C. M. Lieber, J. Phys. D: Appl. Phys. **39**, R387 (2006).
[4]Y. Liu, M. Z. Kauser, M. I. Nathan, P. P. Ruden, S. Dogan, H. Morkoc, S. S. Park, and K. Y. Lee, Appl. Phys. Lett. **84**, 2112 (2004).
[5]Z. L. Wang and J. H. Song, Science **312**, 242 (2006).
[6]X. D. Wang, J. H. Song, J. Liu, and Z. L. Wang, Science **316**, 102 (2007).
[7]Y. Qin, X. D. Wang, and Z. L. Wang, Nature (London) **451**, 809 (2008).
[8]X. D. Wang, J. Zhou, J. H. Song, J. Liu, N. S. Xu, and Z. L. Wang, Nano Lett. **6**, 2768 (2006).
[9]J. H. He, C. L. Hsin, J. Liu, L. J. Chen, and Z. L. Wang, Adv. Mater. **19**, 781 (2007).
[10]C. S. Lao, Q. Kuang, Z. L. Wang, M. C. Park, and Y. L. Deng, Appl. Phys. Lett. **90**, 262107 (2007).
[11]Y. F. Hu, Y. L. Chang, P. Fei, R. L. Snyder, and Z. L. Wang, ACS Nano **4**, 1234 (2010).
[12]Y. F. Hu, Y. Zhang, Y. L. Chang, R. L. Snyder, and Z. L. Wang, "Optimizing the Power Output of a ZnO Photocell by Piezopotential, ACS Nano (2010), DOI: 10.1021/nn1010045.
[13]Y. F. Gao and Z. L. Wang, Nano Lett. **9**, 1103 (2009).
[14]Y. F. Gao and Z. L. Wang, Nano Lett. **7**, 2499 (2007).
[15]Z. Y. Gao, J. Zhou, Y. D. Gu, P. Fei, Y. Hao, G. Bao, and Z. L. Wang, J. Appl. Phys. **105**, 113707 (2009).
[16]K. W. Chung, Z. Wang, J. C. Costa, F. Williamsion, P. P. Ruden, and M. I. Nathan, Appl. Phys. Lett. **59**, 1191 (1991).
[17]J. Zhou, Y. D. Gu, P. Fei, W. J. Mai, Y. F. Gao, R. S. Yang, G. Bao, and Z. L. Wang, Nano Lett. **8**, 3035 (2008).
[18]J. Zhou, P. Fei, Y. D. Gu, W. J. Mai, Y. F. Gao, R. S. Yang, G. Bao, and Z. L. Wang, Nano Lett. **8**, 3973 (2008).
[19]G. A. Maugin, *Continuum Mechanics of Electromagnetic Solids* (North-Holland, Amsterdam, 1988).
[20]T. Ikeda, *Fundamentals of Piezoelectricity* (Oxford University Press, Oxford, 1996).
[21]R. W. Soutas-Little, *Elasticity* (Dover, Mineola, NY, 1999), Vol. XVI, p. 431.
[22]S. M. Sze, *Physics of Semiconductor Devices* (Wiley, New York, 1981).